Chem Biol Drug Des 2007; **69:** 405–412

Research Article

doi: 10.1111/j.1747-0285.2007.00518.x

Hydrophobic Interactions in Complexes of Antimicrobial Peptides with Bacterial Polysaccharides

Hsin H. Kuo[1,2], Celine Chan[1,2], Lori L. Burrows[3] and Charles M. Deber[1,2,*]

[1]*Division of Molecular Structure & Function, Research Institute, The Hospital for Sick Children, Toronto, ON, Canada M5G 1X8*
[2]*Department of Biochemistry, University of Toronto, Toronto, ON, Canada M5S 1A8*
[3]*Department of Biochemistry and Biomedical Sciences, McMaster University, Hamilton, ON, Canada L8N 3Z5*
**Corresponding author: Charles M. Deber, deber@sickkids.ca*

Biofilms of *Pseudomonas aeruginosa* are responsible for chronic lung infections in cystic fibrosis patients, where they are characterized by overproduction of the exopolysaccharide alginate and are recalcitrant to treatment with conventional antibiotics. Cationic antimicrobial peptides (CAPs) are potential alternatives for the treatment of multidrug-resistant *P. aeruginosa*. However, alginate in *P. aeruginosa* biofilms has been proposed to bind these peptides through hydrophobic interactions, consequently reducing their activity [Chan *et al.*, *J Biol Chem* 2004; 279: 38749–38754]. Here we perform biophysical analyses of the interactions of alginate with a series of novel peptide antibiotics (α-CAPs) of prototypic sequence KK-AAA*X*AA-AAA*X*AAWAA*X*AAA-KKKK (where *X* = Phe, Trp or Leu). The hydrophobic interaction interface in alginate was investigated by examining (i) the effects of polysaccharide composition with respect to D-mannuronate and L-guluronate content; (ii) glycan chain length; (iii) α-CAP Trp fluorescence; and (iv) 1-anilinonaphthalene-8-sulfonate fluorescence. The results show that, while M and G residues produce equivalent effects, hydrophobic interactions between alginate and α-CAPs require a minimal glycan chain length. Peptide interactions with alginate are deduced to be mediated by hydrophobic microdomains comprised of pyranosyl C–H groups that are inducible upon formation of α-CAP–alginate complexes due to charge neutralization between the two species.

Key words: Alginate, antimicrobial peptide, biofilm, bacterial polysaccharide, hydrophobic peptide, peptide-saccharide interactions.

Received 17 April 2007, revised 9 May 2007 and accepted for publication 10 May 2007

The onset of chronic endobronchial bacterial infection in patients with the disease cystic fibrosis is often marked by the formation of biofilms by mucoid variants of *Pseudomonas aeruginosa* (1,2), which are characterized by an over-secretion of the high-molecular-weight polysaccharide alginate that serves as the biofilm matrix (3). Alginate is a linear anionic heteropolymer of β-(1 $\rightarrow$ 4)-D-mannuronate and its epimer α-(1 $\rightarrow$ 4)-L-guluronate (4), wherein segments containing repeating D-mannuronate and L-guluronate are referred to as M-blocks and G-blocks, respectively. Alginate is also synthesized by other Gram-negative bacteria including *Azotobacter vinelandii* and *Pseudomonas fluorescens* (5,6) and by brown algae including *Laminaria hyperborea, Ascophyllum nodosum* and *Macrocystis pyrifera* (7).

Studies on the transport of solutes in *P. aeruginosa* biofilms have suggested that alginate may act as a molecular sieve to reduce the diffusion of antibiotics, such as aminoglycosides, macrolides, quinolones and fluoroquinolones (7–12), although whether reduced rates of diffusion can sufficiently account for increased antibiotic resistance remains controversial. In the case of positively charged antibiotics, electrostatic interactions with alginate are thought to limit their transport in biofilms (13) and treatment of the alginate with an alginate-degrading enzyme results in significantly higher antibiotic penetration rates (12).

Our lab has been investigating a novel category of antibiotics (14) and their application toward *P. aeruginosa* biofilms (15). These are a series of synthetic peptides [α-cationic antimicrobial peptides (CAPs)] that consist of a non-amphipathic hydrophobic core sequence AAA*X*AAAAA*X*AAWAA*X*AAA (where the *X* positions represent three copies of the same non-polar residue), with two Lys residues at the N-termini and four Lys residues at the C-termini. These α-CAPs have been shown to insert spontaneously into lipid membranes and to adopt helical conformations when the core hydrophobicity is above an experimentally determined threshold based on the Liu–Deber hydrophobicity scale (16). Insertion into bacterial cell membranes and subsequent disruption of lipid packing serve as the basis of antimicrobial activity for this category of antibiotics.

Hydrophobic sequences such as α-CAPs fold from a disordered conformation in an aqueous environment, into α-helices in a membrane, driven largely by replacement of water-solvated peptide bonds by intramolecular H-bonding in the non-polar environment (17,18). Our laboratory has previously shown that α-CAPs undergo a

similar structural transition when associated with alginate (15), suggesting that alginate is capable of mediating hydrophobic interactions with α-CAPs despite the lack of an obvious membrane-like hydrophobic core in such a water-soluble polysaccharide. We have suggested that alginate from biofilms in effect behaves as an 'auxiliary membrane' that plays a unique protective role toward bacteria by entrapping α-CAPs within the biofilm matrix before they can reach the membranes of the embedded bacterial cells (19).

In the present study, we have investigated the molecular origin of this hydrophobic interface in alginate by examining the effects of alginate composition – e.g. M-block and G-block sequences and glycan chain length – on the secondary structure and fluorescence emission spectra of α-CAPs and by probing the hydrophobic surfaces of alginate using the hydrophobic fluorophore 1-anilinonaphthalene-8-sulfonate (ANS). An understanding of the mechanism that describes hydrophobic interactions between alginate and α-CAPs would serve as the framework for future α-CAP designs as well as in the optimization of the antimicrobial activity of this category of antibiotics toward *P. aeruginosa* biofilms.

Experimental Procedures

Peptide synthesis

Amino acid sequences of α-CAPs studied in the present work are listed in Table 1. The reagents for peptide synthesis, cleavage and purification were 9-fluorenylmethoxycarbonyl (Fmoc)-protected amino acids (Novabiochem, Merck Biosciences AG, Switzerland), [5-(4-Fmoc-aminomethyl-3,5-dimethoxyphenoxy) valeric acid]–polyethylene glycol–polystyrene (PAL–PEG–PS) resin (Applied Biosystems, Foster City, CA, USA), *N,N*-dimethylformaamide (peptide grade; Caledon Laboratories Ltd, Hamilton, ON, Canada), piperidine (Applied Biosystems), methanol (Caledon), *N,N*-diisopropylethylamine (DIEA; Aldrich, St Louis, MO, USA), *O*-(7-azabenzotriazol-1-yl)-1,1,3,3-tetramethyluronium hexafluorophosphate (HATU; Applied Biosystems), diethyl ether (Caledon), triisopropylsilane (TIPS; Aldrich), phenol (Invitrogen, Carlsbad, CA, USA), trifluoroacetic acid (TFA; Aldrich) and acetonitrile (Caledon). The peptides were synthesized via a continuous flow Fmoc solid-phase method on a PerSeptive Biosystems (Foster City, CA, USA) Pioneer peptide synthesizer using the standard cycle as described previously (20). Amino acids were used at fourfold excess, with HATU and DIEA serving as the activator pair. PAL–PEG–PS resin was used to produce an amidated C-terminus. Deprotection and cleavage of peptides were carried out in a solution of 88% TFA, 5% phenol, 5% water and 2% TIPS for 2 h, constant shaking at room temperature, followed by cold diethyl ether precipitation and lyophilization. Purification of the peptides was carried out on a reverse-phase C4 preparative HPLC (21.2 × 250 mm, 300 Å), using a linear gradient of acetonitrile in 0.1% TFA. Concentrations of peptides were determined in duplicate using the micro-bicinchoninic acid protein assay.

Table 1: Amino acid sequences of selected α-CAPs and their designations

α-CAP	Amino acid sequence[a]	MW (Da)
X = Phe	**KK**AAAFAAAAAFAAWAAFAAA**KKKK**-NH_2	2480
X = Trp	**KK**AAAWAAAAAWAAWAAWAAA**KKKK**-NH_2	2597
X = Leu	**KK**AAALAAAAALAAWAALAAA**KKKK**-NH_2	2378

[a]Charged residues are shown in boldface; guest X-residues and the Trp fluorescence marker are underlined.

Extraction of M-block and G-block sequences

Alginate sequences enriched in G-block ($Alg_{G\text{-}G}$) or M-block ($Alg_{M\text{-}M}$) were prepared using a procedure adapted from a previously described method (21). Alginate (Pronova, Sandvika, Norway) was subjected to partial acid hydrolysis at pH 2.0, 90 °C for 2 h to hydrolyze the axial–equatorial and equatorial–axial glycosidic linkages between D-mannuronate and L-guluronate, while preserving the equatorial–equatorial β-(1 → 4) and axial–axial α-(1 → 4) glycosidic linkages in M-blocks and G-blocks, respectively. The suspension was cooled and centrifuged to recover residue containing M-block and G-block. The residue was resuspended in distilled water, neutralized with ammonium bicarbonate and lyophilized. The dried residue was dissolved in 0.1 M of NaCl to make a 1% solution. The pH was slowly adjusted to 2.8 by the dropwise addition of 25 mM HCl, to precipitate alginate consisting of mainly G-block ($Alg_{G\text{-}G}$), while alginate consisting of mainly M-block ($Alg_{M\text{-}M}$) remained in the supernatant. $Alg_{M\text{-}M}$ and the resuspended $Alg_{G\text{-}G}$ were passed through a Centricon (Millipore, Billerica, MA, USA) centrifugal filter (3-kDa cut-off) to remove salt and low-molecular-weight oligosaccharides. The average degree of polymerization (DP) of $Alg_{M\text{-}M}$ and $Alg_{G\text{-}G}$ were determined using the Somogyi–Nelson assay for reducing sugars (22), using D-galacturonate as the standard. The average DP was calculated by dividing the total uronate content by the number of reducing ends. The homogeneity of M-blocks and G-blocks were assessed via circular dichroism spectroscopy using a previously described method (23).

Circular dichroism spectroscopy

Circular dichroism spectra of peptides were recorded on a Jasco-810 spectro-polarimeter (Jasco Inc., Easton, MD, USA) using a 1-cm path-length quartz cell at 25 °C. Each spectrum was the average of three scans with buffer and alginate background subtracted. Peptide concentrations were typically 5 μM and spectra were collected in 1 mM 2-(*N-Morpholino*)ethanesulfonic acid (MES) buffer (pH 5.5) and in 0.1 mg/mL alginate, $Alg_{G\text{-}G}$ or $Alg_{M\text{-}M}$ solutions. Where applicable, the molar ellipticity at 222 nm is reported.

Tryptophan fluorescence emission

Fluorescence emission spectra of peptide Trp residues were recorded on a Hitachi F-400 Photon Technology International C-60 fluorescence spectrometer (Photon Technology International, London, ON, Canada) at room temperature, using semimicro quartz cuvettes of 1 mL (10-mm excitation path length and 10-mm emission path length) (Hellman, Concord, ON, Canada). The excitation wavelength was 280 nm, and the emission spectra were recorded from 300 to 400 nm. Spectra were collected with a step size of 1 nm with an average of three cycles. Peptide concentrations were 5 μM in 1 mM pH 5.5 MES buffer or buffer with 0.1 mg/mL of alginate, $Alg_{G\text{-}G}$ or $Alg_{M\text{-}M}$. Blue shift ($\Delta\lambda_{max}$) of Trp is reported as the difference of the wavelength of emission maxima of Trp in aqueous buffer to alginate solutions.

ANS fluorescence measurements

Ten μM of ANS (Aldrich) was added to alginate of concentrations ranging from 0.5 to 10 mg/mL; 2.5–100 μM of peptides; or increasing peptide concentration at 0.5, 1.0 and 2.0 mg/mL alginate. Fluorescence intensities at 500 nm were measured using an excitation of 375 nm in 1 mM pH 5.5 MES buffer at room temperature following a 5-min incubation period (I_p), and subtracted by the background fluorescence of ANS in distilled water (I_o). Maximum fluorescence intensity of ANS was determined by the addition of 10 mM sodium lauryl sulfate (SLS) (I_{max}). The percent emission of ANS (I_{ANS}) localized to hydrophobic regions was therefore calculated by: $100 \times (I_p - I_o)/(I_{max} - I_o)$. The readings reported are the average of three experiments. Experiments were carried out using both non-*O*-acetylated alginate (Pronova) and *O*-acetylated alginate that was purified from *P. aeruginosa* FRD1 strains as described previously (24).

Chromatography of oligo-uronates

One-milliliter solutions of either $Alg_{M\text{-}M}$ or $Alg_{G\text{-}G}$ in 50 mM Tris–HCl pH 7.0 were incubated with 10 μg of alginate lyase from *Flavobacterium* sp. (Sigma Aldrich, St Louis, MO, USA). The reactions were carried out at 25 °C and terminated by heat inactivation after 10, 20, 30 and 60 min, yielding a series of progressively shorter unsaturated poly-β-(1 $\rightarrow$ 4)-D-mannuronate or poly-α-(1 $\rightarrow$ 4)-L-guluronate. Gel filtration of the unsaturated poly-uronates was performed on a Bio-Gel P-6 column (BioRad, Hercules, CA, USA) (3 $\times$ 100 cm), eluted with 50 mM ammonium bicarbonate running at 20 mL/h, and fractionated into 5-mL aliquots. Unsaturated uronates in each fraction were detected via absorbance at 235 nm. Each peak was pooled and lyophilized to remove ammonium bicarbonate. Poorly resolved fractions were collected and further separated on a Bio-Gel P-10 column as described above. Finally, the concentrations of uronates in each fraction were determined using the carbazole assay (25). DP for each fraction was determined from the molecular weights detected by negative-ion mode Electrospray ionization (ESI)–mass spectrometry. Average DP in fractions that were undetectable by ESI–mass spectrometry was determined by the Somogyi–Nelson method (22).

Results

M-blocks and G-blocks of alginate induce helical conformations in α-CAPs

The homogeneity of $Alg_{M\text{-}M}$ and $Alg_{G\text{-}G}$ sequences extracted from alginate was assessed using circular dichroism (CD) spectroscopic techniques as previously described (23). The frequency of α-L-guluronate repeats (G-block) was estimated to be 0.92 in $Alg_{G\text{-}G}$ sequences, while the frequency of β-D-mannuronate repeats (M-block) was estimated to be 0.86 in $Alg_{M\text{-}M}$ sequences. The sequence length or the average DP (DP_{avg}) for $Alg_{M\text{-}M}$ and $Alg_{G\text{-}G}$ determined by the Somogyi–Nelson method was around 28 and 22 units, respectively. While sequences of higher homogeneity are, in principle, obtainable, such preparations would likely be accompanied by a further reduction in DP_{avg}, which is undesirable in maintaining an ideal interaction surface with the α-CAPs.

The CD spectra of selected α-CAPs (X = Phe, X = Trp and X = Leu; Table 1) exhibited typical α-helical profiles with characteristic minima at 222 and 208 nm, in both $Alg_{M\text{-}M}$ and $Alg_{G\text{-}G}$ sequences extracted from alginate (Figure 1). The molar ellipticities of α-CAPs in both cases were significantly lower on average than the starting

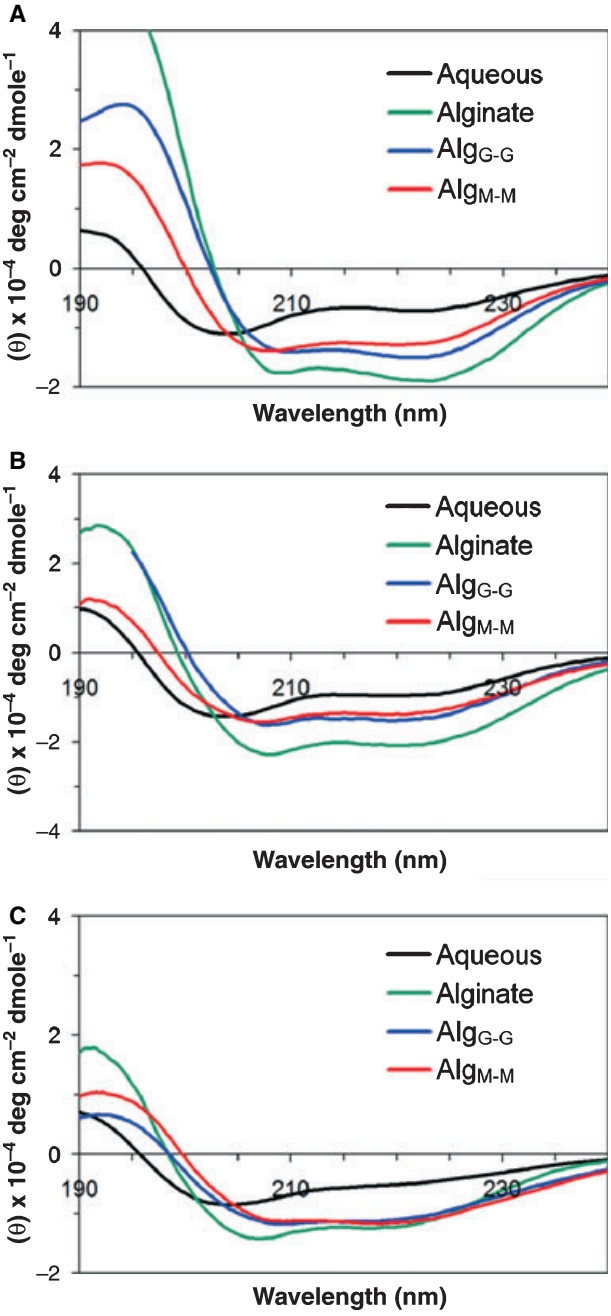

Figure 1: CD spectra of selected α-CAPs in $Alg_{M\text{-}M}$ and $Alg_{G\text{-}G}$ extracted from alginate. (A) X = Phe; (B) X = Leu; (C) X = Trp. Peptide concentrations were typically 5 μM. Spectra of peptides were recorded in aqueous buffer, in alginate, in $Alg_{G\text{-}G}$ and in $Alg_{M\text{-}M}$, as indicated on the diagram. $Alg_{G\text{-}G}$ and $Alg_{M\text{-}M}$ are alginate sequences enriched in repeating α-L-guluronate (G-block), and β-D-mannuronate (M-block), respectively. Solutions were buffered in pH 5.5 MES. Spectra reported are the average of three scans, corrected for the buffer and alginate background.

alginate from which $Alg_{M\text{-}M}$ and $Alg_{G\text{-}G}$ were extracted, which initially indicates that the M-block and G-block sequences may cooperatively induce helical conformation in α-CAPs. However, no significant changes to the CD profile of α-CAPs were observed by mixing $Alg_{M\text{-}M}$ and $Alg_{G\text{-}G}$ in various ratios (data not shown), suggesting that the difference in molar ellipticity is mainly due to the starting alginate having a higher molecular weight to accommodate additional binding of α-CAPs. Minor differences were observed between the spectra of selected α-CAPs in complex with $Alg_{M\text{-}M}$ and with $Alg_{G\text{-}G}$, notably in the 222 nm minima, which are generally more pronounced in the spectra recorded in $Alg_{G\text{-}G}$. This shift in molar ellipticity may be due to $Alg_{G\text{-}G}$ sequences exhibiting a slightly greater binding affinity toward α-CAPs, although presently contributions from variations in sequence length and homogeneity between $Alg_{M\text{-}M}$ and $Alg_{G\text{-}G}$ cannot be excluded. Due to these variations, precise comparisons of the interaction affinity between G-block and M-block sequences of alginate with α-CAPs are limited. In spite of this, the ability to interact and subsequently induce α-helical conformation in α-CAPs is clearly not an effect exclusive to either type of sequence.

M-block and G-block sequences of alginate induce blue shifts in Trp fluorescence emission maxima of α-CAPs

A Trp residue is present in the hydrophobic core of α-CAPs to serve as a probe for changes in the local environment of the peptides. It was previously shown that α-CAPs exhibited a shift in their Trp emission maxima to a lower wavelength (blue shift) with the addition of alginate, concomitant with the induction of α-helical conformation (15). The Trp fluorescence emission maxima for selected α-CAPs (X = Phe, X = Trp and X = Leu) in buffer were typically 350 nm, as previously reported for a Trp residue in aqueous environments (26), whereas upon the addition of alginate, blue shifts of approximately 10–15 nm were consistently observed (Table 2), indicating that the indole ring has been localized to a more hydrophobic environment in alginate (27). As similar shifts in emission maxima were observed when either the $Alg_{M\text{-}M}$ or $Alg_{G\text{-}G}$ block sequences of alginate were added to the peptides, and in concert with the fact that both $Alg_{M\text{-}M}$ and $Alg_{G\text{-}G}$ were individually sufficient to induce conformational changes in α-CAPs, both of these structural units of alginate must exhibit a considerable degree of hydrophobic character.

Table 2: Alginate-induced blue shifts in Trp fluorescence emission maxima of α-CAPs

	Trp $\Delta\lambda_{max}$ (nm)[a]		
α-CAP	Alginate[b]	$Alg_{M\text{-}M}$[c]	$Alg_{G\text{-}G}$[d]
X = Phe	15	13	15
X = Trp	9	8	8
X = Leu	16	14	15

Emission spectra were recorded with an excitation wavelength of 280 nm. Uncertainty in the wavelength maxima is estimated as ±1 nm.
[a]$\Delta\lambda_{max}$ reported as (λ_{max} buffer−λ_{max} alginate).
[b]Native alginate containing both M-blocks and G-blocks.
[c]Extracted alginate sequences enriched in M-blocks.
[d]Extracted alginate sequences enriched in G-blocks.

Alginate is intrinsically hydrophilic but forms hydrophobic complexes with α-CAPs

While Trp fluorescence suggested that alginate possesses hydrophobic components, contributions from other non-polar amino acid residues of the peptide cannot be excluded from the observed spectroscopic changes. In order to decouple the effects of other side chains in α-CAPs, the environment-sensitive spectroscopic property of ANS was employed to determine whether hydrophobic surfaces exist in alginate in the absence of α-CAPs. ANS is a hydrophobic fluorescent probe commonly used in the determination of critical micelle concentrations of surfactants (28) and in the detection of non-polar surfaces in proteins, protein aggregates and supramolecular assemblies (29–31).

Two types of alginate were tested: non-*O*-acetylated alginate of kelp origin and *O*-acetylated alginate of bacterial (*P. aeruginosa*) origin. The percent emission intensity of ANS (I_{ANS}) showed no significant increase above basal fluorescence in aqueous buffer with increasing non-*O*-acetylated alginate concentrations (Figure 2A),

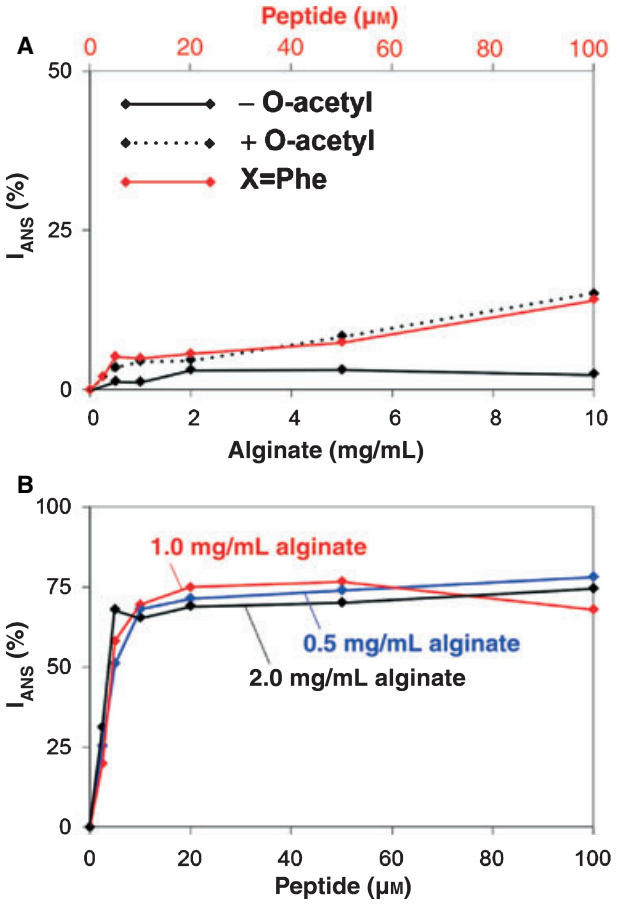

Figure 2: ANS fluorescence in alginate and in alginate-α-CAP complexes. (A) I_{ANS} at increasing concentrations of *O*-acetylated *P. aeruginosa* alginate; non-*O*-acetylated kelp alginate; and the α-CAP X = Phe. (B) I_{ANS} at increasing X = Phe concentrations in complex with alginate at indicated concentrations. I_{ANS} values are reported as percent of maximum emission (I_{max}) observed when ANS is in the presence of SLS micelles.

suggesting that alginate does not possess intrinsic hydrophobic domains conducive to ANS binding. The presence of *O*-acetyl groups in alginate from *P. aeruginosa* resulted in a discernibly higher I_{ANS} (Figure 2A). However, even at the highest concentration of alginate compatible with spectroscopic measurements, I_{ANS} for both non-*O*-acetylated and *O*-acetylated alginate remained only a fraction of that observed in micellar or lipid systems. Thus, despite the ability of alginate to induce Trp blue shifts and structural transitions upon binding α-CAPs, it is itself an essentially hydrophilic polymer. The presence of *O*-acetyl groups may supplement – but are not necessary – for driving hydrophobic interactions of alginate with α-CAPs.

When the α-CAP X = Phe was added to ANS in increasing concentrations, a small increase in I_{ANS} was observed, likely due to the intrinsic hydrophobic character of this peptide (Figure 2A). I_{ANS} at relatively high peptide concentration was slightly above the basal level (aqueous buffer). However, I_{ANS} increased significantly upon the addition of X = Phe to 0.5 mg/mL alginate, reaching a plateau at around 20 μM peptide (Figure 2B). I_{ANS} was not enhanced by further additions of peptide or alginate, which suggests that all ANS molecules in the system were interacting with the alginate–peptide complex. Similar results were obtained when the peptide X = Leu was added to alginate (H.H. Kuo and C.M. Deber, unpublished).

I_{ANS} observed in the alginate–peptide system is noticeably lower than the maximum emission intensity (I_{max}) of ANS in SLS micelles, which initially indicates that alginate may be partially quenching ANS fluorescence. Control experiments for the quenching of I_{ANS} by alginate showed that alginate up to 2 mg/mL did not significantly quench the fluorescence of ANS in SLS micelles (Figure 3). Therefore, low levels of I_{ANS} in alginate are due to the lack of hydrophobic sites conducive for ANS binding, and not due to quenching of bound ANS. The lower I_{ANS} observed in the alginate–peptide complex compared with micellar system is likely due to less effective shielding of water molecules in the alginate–peptide complex. Furthermore, in the presence of non-antimicrobially active peptides that are cationic and hydrophilic, no increase in I_{ANS} was observed (data not shown). Initially, this suggested that ANS binds to hydrophobic α-CAPs in alginate, rather than alginate specifically. Nevertheless, ANS did not appear to bind to α-CAPs alone; the increase in I_{ANS} is unique to α-CAPs when in complex with alginate.

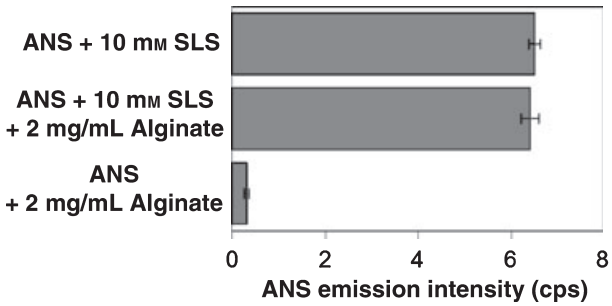

Figure 3: Control for ANS fluorescence quenching by alginate. Maximum ANS emission intensity (I_{max}) recorded with 10 μM ANS in 10 mM sodium lauryl sulfate (SLS). No quenching of I_{max} by alginate up to 2 mg/mL was observed.

Induction of helical conformations in α-CAPs is dependent on the length of the alginate glycan chain

Oligo-L-guluronates and oligo-D-mannuronates fractionated from $Alg_{G\text{-}G}$ and $Alg_{M\text{-}M}$ were examined by CD spectroscopy for their ability to induce an α-helical conformation in α-CAPs. The average molar ellipticity at 222 nm ($\theta_{222\ nm}$) of X = Phe showed no significant increase in the presence of oligo-L-guluronates of 3–6 DP (Figure 4), indicating that low-molecular-weight oligo-uronates of alginate do not induce secondary structure in hydrophobic peptides. In α-CAPs, there are a total of six Lys that are distributed at the C-termini and N-termini. Small oligo-uronates which form ion pairs with Lys side chains are not expected to impose steric restrictions on the conformation of the peptide backbone and therefore no structure induction was observed with either oligo-L-guluronates or oligo-D-mannuronates of lower than 6 DP. In the presence of oligo-L-guluronates of 7 DP or longer, the X = Phe peptide exhibited a progression toward an α-helical fold, with $\theta_{222\ nm}$ reaching a plateau at around 12 DP. In the presence of oligo-D-mannuronates, a similar profile of $\theta_{222\ nm}$ as a function of DP was observed. In both cases, the conformation of X = Phe was sensitive to the mixing ratio of peptide to oligo-uronates of 7–12 DP. In this range of DP, large shifts in $\theta_{222\ nm}$ were typical in both oligo-L-guluronates and oligo-D-mannuronates, and visible aggregates were often observed. At a higher DP (15+), X = Phe adopted a more consistent and stable α-helical fold.

Discussion

Peptide interactions with M-blocks versus G-blocks of alginate

The notion that alginate in biofilms may display hydrophobic properties initially appears contradictory, given that sugars are generally water soluble and contain numerous free hydroxyl groups. However, there have been a number of suggestions from past studies that

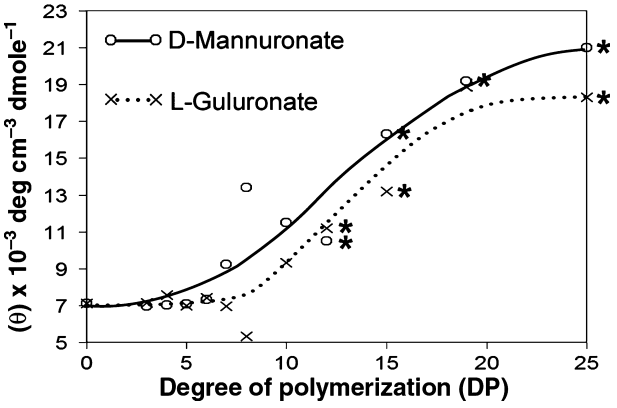

Figure 4: Helical content of α-CAP X = Phe as a function of alginate DP. Molar ellipticity [θ] recorded at 222 nm. Solid line: $[\theta]_{222\ nm}$ of X = Phe in oligo-D-mannuronate as a function of increasing DP. Dotted line: $[\theta]_{222\ nm}$ of X = Phe in oligo-D-guluronate as a function of increasing DP. '*' denotes fractions for which the average DP is reported.

polysaccharides, by adopting certain conformations, exhibit hydrophobic character (32,33). In fact, a hydrophobic index based on surface area of pyranosyl C–H groups for monosaccharides has been proposed, which listed mannose – the neutral equivalent of mannuronate in alginate – as the most hydrophobic of hexoses (34). Blue shifts in the emission of Trp have also been observed when a pyranosyl ring and the indole ring of Trp stack together, thereby excluding water molecules from the side chain (35). Such an interaction is commonly observed in protein–carbohydrate complexes (36,37), including alginate binding proteins (38).

We previously postulated that the interaction of α-CAPs with alginate would occur in a similar manner, where D-mannuronate would interact with non-polar side chains through its hydrophobic surface which in this mannose analog is comprised of four aligned C–H groups (15). However, while the L-guluronate rings lack a comparable hydrophobic face in the sense that the C–H bonds (C_1, C_3 and C_4) are equatorial rather than axial, we observed here that Trp blue shifts were of similar magnitude in $Alg_{M\text{-}M}$ and $Alg_{G\text{-}G}$ blocks, indicating that the $Alg_{G\text{-}G}$ sequence must also contain significant non-polar surfaces. This finding is likely attributable to the conformation of G-blocks, which are distinct from M-blocks in their linkage modes. Thus, M-blocks are di-equatorially linked flat and extended structures, whereby the axial C–H groups are exposed. In contrast, G-blocks are comparatively compact structures that are diaxially linked, such that the L-guluronate rings are 'stacked' and hydrophobic surfaces are likely formed by the equatorial C–H groups instead (Figure 5A).

In some bacterial alginates, where both M-block and G-block units are present, the G-block may have a more dominant role in mediating structural transitions in α-CAPs and subsequently restrict their transport though the biofilm. Bacterial M-blocks may also carry *O*-acetyl groups (39) that can potentially hinder the accessibility to the carboxylate groups that are likely necessary for the initial α-CAP binding. However, in *P. aeruginosa* alginate specifically, where G-blocks do not exist, the blocking activity likely involves a delicate balance between the interaction interface provided by M-blocks, and sequences with alternating α-L-guluronate and β-D-mannuronate (MG-blocks).

Role of glycan chain length and charge neutralization

Lysines at the termini of α-CAPs normally serve to prevent peptide–peptide aggregation through the presence of high local concentrations of positive charge (40). Neutralization of the Lys residues by alginate glycan chains could therefore lead to solubility issues with these peptides. At a 1:1 ratio of negatively charged (carboxylate) to positively charged (Lys) groups, visible aggregates are typically observed in mixtures of α-CAPs with alginate. This effect is not exclusive to the binding of α-CAPs, but generally true for the interaction of alginate with other polypositively charged polymers, which depending on the concentration ratio (charge group ratio), can result in a spectrum of phase transitions from gels to aggregates (41,42). Similarly, by decreasing the length of alginate glycan chains, the potential number of α-CAPs each alginate molecule can accommodate is significantly reduced. At *ca.* 7–12 DP, each glycan chain can feasibly accommodate one or two peptides at most, before reaching 1:1 charge saturation. In essence, as the length of the alginate glycan chain is increased, a hydrophobic interface that mediates secondary structure induction of α-CAPs becomes possible. Fundamentally, the induction of the α-helical conformation may be due to the bound peptides reaching a solubility limit due to charge neutralization, but at the same time, extensive peptide–peptide aggregation is avoided due to charge repulsions between alginate glycan chains. By comparison, in membranes, infinite assemblies of peptides are likely avoided due to the solvation effects of the lipid hydrocarbon tails, where the extent of peptide oligomerization is controlled by the equilibrium between peptide–peptide and peptide–lipid hydrophobic interactions.

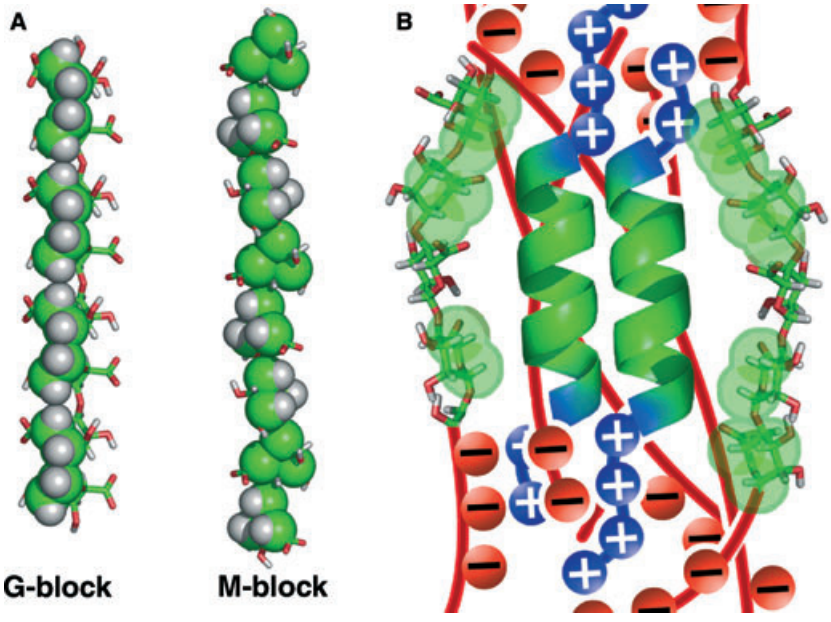

Figure 5: Hydrophobic components of M-block and G-block of alginate. (A) Model of β-(1 → 4)-D-mannuronate (M-block) and α-(1 → 4)-L-guluronate (G-block) tetrasaccharides. Hydrophobic surface as represented by clusters of pyranosyl C–H groups is shown as a space-filling overlay. (B) Schematic representation of the α-CAP–alginate complex formed by the interaction of C–H clusters with the hydrophobic peptide surface.

Alginate traps α-CAPs in peptide-induced hydrophobic microdomains

While it is generally believed that ANS binds through its hydrophobic naphthalene moiety, earlier reports indicate that electrostatic interaction with the negatively charged sulfonate group can mediate binding of the hydrophobic dye to positively charged residues in soluble proteins (43,44). However, as the positively charged side chains α-CAPs are effectively neutralized by the carboxylate groups of alginate, the peptide–alginate complex lacks charged groups that can participate in ion pair interactions with ANS. Hence, it appears that hydrophobic effects, rather than charge–charge interactions, drive the binding of ANS to the alginate–peptide complex.

A study using the neutral fluorophore pyrene with alginate suggested the presence of hydrophobic regions within alginate, but only at concentrations approaching the solubility limit of alginate (45). Thus, while both M-blocks and G-blocks of alginate contain 'hydrophobic regions', their intrinsic hydrophobicity at typical concentrations is relatively weak as they would be comprised of primarily C–H groups of the pyranosyl rings and the occasional *O*-acetyl groups. Consistent with this scenario, alginate itself did not appear to bind strongly to the hydrophobic probe ANS, which suggests that the presence of negatively charged carboxylate groups likely masks hydrophobic contributions from C–H groups. Thus, as the binding of ANS to α-CAP–alginate complexes suggests, the hydrophobic surfaces inherent in alginate become accessible under the conditions where polysaccharide carboxylate groups are locally neutralized and continuous clusters of C–H groups become exposed along the glycan chain, forming hydrophobic microdomains in the process of binding the positively charged α-CAPs (Figure 5B).

The detailed nature of hydrophobic contacts in the α-CAP–alginate complex remains to be determined. Previous studies observed that α-CAPs form oligomers in alginate (15) and therefore ANS may be primarily bound to these higher order assemblies. On the other hand, α-CAPs may 'bridge' nascent alginate glycan chains via Lys side chains, due to peptide–peptide self-association. It is thus possible that ANS may intercalate between the alginate glycan chains and α-CAPs. Regardless of the precise binding sites for ANS, it is clear that the putative 'hydrophobic microdomains' that induce both Trp blue shifts and helical conformations of α-CAPs are not intrinsic to alginate, but appear to be induced upon the binding of α-CAPs to alginate.

Conclusion

Our overall results suggest that diffusion of α-CAPs in biofilms is reduced due to the cascade of electrostatic and hydrophobic interactions as the peptides attempt to traverse the alginate barrier as α-helical bundles. Although increasing the average core hydrophobicity of the peptides can improve their antimicrobial activity while allowing them to remain soluble in detergents or lipids, as observed in a previous study (14), this approach is likely to shift the equilibrium toward peptide–peptide interactions in the weakly hydrophobic alginate, ultimately resulting in peptide aggregation and inactivation. In essence, then, the qualities that constitute a potent antimicrobial peptide are simultaneously detrimental with regard to maintaining solubility and antimicrobial activity in alginate; thus, a balanced trade-off of antimicrobial activity in favor of alginate permeability may be more efficacious in future designs of peptides that act against *P. aeruginosa* biofilms. In this context, the present work provides a novel explanation for the observed resistance of biofilms to CAPs. As further details of peptide interactions with alginate emerge, suitable manipulation of peptide hydrophobicity, charge and length can potentially produce peptides which more effectively penetrate the alginate barrier and kill *P. aeruginosa*.

Acknowledgments

This work was supported, in part, by grants to L.L.B. and C.M.D. from the Canadian Institutes of Health Research (CIHR). C.C. was the recipient of a University of Toronto Fellowship. H.H.K. held a Research Training Award from the Research Institute, Hospital for Sick Children.

References

1. Deretic V., Schurr M.J., Yu H. (1995) *P. aeruginosa* mucoidy and the chronic infection phenotype in cystic fibrosis. Trends Microbiol;3:351–356.
2. Singh P.K., Schaefer A.L., Parsek M.R., Moninger T.O., Welsh M.J., Greenberg E.P. (2000) Quorum-sensing signals indicated that cystic fibrosis lungs are infected with bacterial biofilms. Nature;407:762–764.
3. Costerton J.W., Stewart P.S., Greenberg E.P. (1999) Bacterial biofilms: a common cause of persistent infections. Science;284: 1318–1322.
4. Gacesa P. (1998) Bacterial alginate biosynthesis-recent progress and future prospects. Microbiology;144:1133–1143.
5. Clementi F. (1997) Alginate production by *Azotobacter vinelandii*. Crit Rev Biotechnol;17:327–361.
6. Govan J.R., Fyfe J.A., Jarman T.R. (1981) Isolation of alginate-producing mutants of *Pseudomonas fluorescens*, *Pseudomonas putida*, and *Pseudomonas mendocina*. J Gen Microbiol;125:217–220.
7. Draget I.K., Smidsrod O., Skjak-Braek G. (2005) Alginates from algae. In: Steinbuchel A., Rhee S.K., editors. In Polysaccharides and Polyamides in the Food Industry. Properties, Production and Patents.
8. Hoyle B.D., Alcantara H., Costerton J.W. (1992) *Pseudomonas aeruginosa* biofilm as a diffusion barrier to piperacillin. Antimicrob. Agents Chemother;36:2054–2056.
9. Kumon H., Tomochika K., Matunaga T., Ogawa M., Ohmori H. (1994) A Sandwich cup method for the penetration assay of antimicrobial agents through the *Pseudomonas* exopolysaccharides. Microbiol. Immunol.;38:615–619.
10. Shigeta M., Tanaka G., Komatsuzawa H., Sugai M., Suginaka H., Usui T. (1997) Permeation of antimicrobial agents through *Pseudomonas* aeruginosa biofilms: a simple method. Chemother; 43:340–345.
11. Suci P., Mittelman M.W., Yu F.P., Geesy G.G. (1994) Investigation of ciprofloxacin penetration into *Pseudomonas aeruginosa* biofilms. Antimicrob. Agents Chemother;38:2125–2133.

12. Hatch R.A., Schiller N.L. (1998) Alginate lyase promotes diffusion of aminoglycosides through the extracellular polysaccharide of mucoid *Pseudomonas aeruginosa*. Antimicrob. Agents. Chemother;42:974–977.
13. Nichols W.W., Dorrington S.M., Slack M.P. (1988) Inhibition of tobramycin diffusion by binding to alginate. Antimicrob. Agents. Chemother;32:518–523.
14. Stark M., Liu L.P., Deber C.M. (2002) Cationic hydrophobic peptides with antimicrobial activity. Antimicrob Agents Chemother;46:3585–90.
15. Chan C., Burrows L.L., Deber C.M. (2004) Helix induction in antimicrobial peptides by alginate in biofilms. J Biol Chem;279: 38749–38754.
16. Deber C.M., Liu L.-P., Wang C., Goto N., Reithmeier R.A.F. (2002) The Hydrophobicity threshold for peptide insertion into membranes. In: Simon S.A., McIntosh T.J., (eds). Peptide-Lipid Interactions, Current Topics in Membranes; 52:459–473.
17. White S.H., Wimley W.C. (1999) Membrane protein folding and stability: Physical principles. Annu Rev Biophys Biomol Struct;28:319–365.
18. Popot J.L., Engelman D.M. (1990) Membrane protein folding and oligomerization: the two-stage model. Biochemistry;29:4031–4037.
19. Chan C., Burrows L.L., Deber C.M. (2005) Alginate as an auxiliary bacterial membrane: binding of membrane-active peptides by polysaccharides. J Pept Res;65:343–351.
20. Liu L.P., Deber C.M. (1997) Anionic phospholipids modulate peptide insertion into membranes. Biochemistry;36:5476–5482.
21. Haug A., Larsen B., Simgsrod O. (1962) Quantitative determination of uronic acid composition of alginate. Acta Chem Scand;16:1908–1918.
22. Green F., Clausen C.A., Highley T.L. (1989) Adaptation of the Nelson-Somogyi reducing sugar-assay to a microassay using microtiter plates. Anal Biochem;182:197–199.
23. Donati I., Gamini A., Skjak-Braek G., Vetere A., Campa C., Coslovi A., Paoletti S. (2003) Determination of the diadic composition of alginate by means of circular dichroism: a fast and accurate improved method. Carbohydr Res;338:1139–1142.
24. Pedersen S.S., Espersen F., Hoiby N., Shaund G.H. (1989) Purification, characterization, and immunological cross-reactivity of alginates produced by mucoid *Pseudomonas aeruginosa* from patients with cystic fibrosis. J Clin Microb;27:691–699.
25. Kosakai M., Yoshizawa Z. (1979) A partial modification of the carbazole method of Bitter and Muir for quantification of hexuronic acids. Anal Biochem;93:295–298.
26. Burstein E.A., Vedenkina N.S., Ivkova M.N. (1974) Fluorescence and the location of tryptophan residues in protein molecules. Photochem. Photobiol;18:263–279.
27. Lakowicz J.R. (1999) Principles of Fluorescence Spectroscopy. New York: Academic.
28. Abuin E.B., Lissi E.A., Aspee A., Gonzalez F.D., Varas J.M. (1997) Fluorescence of 8-anilinonaphthalene-1-sulfonate and properties of sodium dodecyl sulfate micelles in water-urea mixtures. J Colloid Interface Sci;186:332–338.
29. Gosline J.M., Yew F.F., Weis-Fogh T. (1975) Reversible structural changes in a hydrophobic protein, elastin, as indicated by fluorescence probe analysis. Biopolymers;14:1811–1826.
30. De Campos Vidal B. (1978) The use of the fluorescent probe 8-anilinonaphthalene sulfate (ANS) for collagen and elastin histochemistry. J Histochem Cytochem;26:196–201.
31. Salemi Z, Hosseinkhani S, Ranjbar B, Nemat-Gorgani M. (2006) Interaction of native and apo-carbonic anhydrase with hydrophobic adsorbents: A comparative structure-function study. J Biochem Mol Biol;39:636–641.
32. Neal J.L., Goring D.A. (1970) Hydrophobic folding of maltose in aqueous solution. Canadian J Chemistry;48:3745–3747.
33. Morris C.J.O.R. (1977) The three essential criteria. Trends in Biochem Sci;1:N16.
34. Masanobu J., Yuki Y. (1985) Hydrophobic nature of sugars as evidenced by their differential affinity for polystyrene in aqueous media. Chem Mat Sci;14:891–902.
35. Vázquez-Ibar J.L., Guan L., Weinglass A. B., Verner G., Gordillo R, Ronald Kaback H. (2005) Sugar Recognition by the lactose permease of *Escherichia coli*. J Biol Chem;297:49214–49221.
36. Spurlino J.C., Rodseth L.E., Quiocho F.A. (1992) Atomic interactions in protein-carbohydrate complexes. Tryptophan residues in the periplasmic maltodextrin receptor for active transport and chemotaxis. J. Mol. Biol;226:15–22.
37. Quiocho F.A., Spurlino J.C., Rodseth L.E. (1997) Extensive features of tight oligosaccharide binding revealed in high-resolution structures of the maltodextrin transport/chemosensory receptor. Structure;5:997–1015.
38. Mishima Y., Momma K., Hashimoto W., Mikami B., Murata K. (2003) Crystal structure of AlgQ2, a macromolecule (alginate)-binding protein of *Sphingomonas sp*. A1, complexed with an alginate tetrasaccharide at 1.6 A resolution. J Biol Chem; 278:6552–6559.
39. Skjak-Braek G., Larsen B., Grasdalen H. (1986) Monomer sequence and acetylation pattern in some bacterial alginate. Carbohydr Res;154:239–250.
40. Liu L.P., Deber C.M. (1998) Guidelines for membrane protein engineering derived from de novo designed model peptides. Biopolymers;47:41–62.
41. Hoffman A.S. (2001) Hydrogels for biomedical applications. Ann N.Y. Acad Sci;944:62–73.
42. Meera G., Abraham T.E. (2006) Polyanionic hydrocolloids for the intestinal delivery of protein drugs: alginate-chitosan – a review. J Control Release;114:1–14.
43. Kirk W.R., Kurian E., Prendergast F.G. (1996) Characterization of the sources of protein-ligand affinity: 1-sulfonato-8-anilinonapthalene binding to intestinal fatty acid binding protein. Biophys J;70:69–83.
44. Matulis D., Lovrien R. (1998) 1-Anilino-8-napthalene sulfonate anion-protein binding depends primarily on ion pair formation. Biophys J;74:422–429.
45. Neumann M.G., Schmitt C.C., Iamazaki E.T. (2003) A fluorescence study of the interactions between sodium alginate and surfactants. Carbohydr Res;338:1109–1113.